ARTICLE

Certified Multi-Fidelity Digital Twins for Soluble Gas-Kick Transients: Reachability-Bounded Alarm Integrity and Real-Time Risk Quantification

Muhammad Afiq[1] and Syed Farhan[2]

[1]Universiti Malaysia Perlis, Pauh Putra Campus, Jalan Kangar–Arau, 02600 Arau, Perlis, Malaysia
[2]Universiti Sultan Zainal Abidin, Kampus Gong Badak, Jalan Sultan Mahmud, 21300 Kuala Terengganu, Terengganu, Malaysia

Abstract

Drilling operations routinely operate within narrow pressure margins where small transient disturbances can produce disproportionate safety consequences. Gas influx events are especially challenging because the surface observables used for monitoring, including wellhead pressure and pit-volume change, are shaped by nonlinear multiphase transport, compressibility, slip, thermal gradients, and, in synthetic or oil-based drilling fluids, methane dissolution that can temporarily conceal gas mass. This paper develops a certified digital-twin methodology aimed at alarm integrity rather than point prediction. The core contribution is a multi-fidelity modeling and analysis stack that produces real-time outer bounds on safety-critical indicators under bounded uncertainty in influx, hydraulics, and thermodynamic partitioning between free and dissolved gas. A physics-consistent one-dimensional annular model is formulated as a constrained dynamical system with explicit dissolved-gas inventory and smooth phase-partition closure. Uncertainty is propagated through reachability analysis that computes guaranteed enclosures of indicator trajectories, enabling quantified false-alarm and missed-detection risk without assuming perfect calibration. To achieve field-feasible runtime, the method couples conservative interval-based propagation for stiff thermodynamic components with reduced-order linear surrogates learned from local linearizations, while preserving certification by bounding surrogate residuals. The resulting digital twin supplies time-varying alarm thresholds, integrity metrics, and decision support signals that adapt to operating conditions and uncertainty magnitude. Computational studies across circulation regimes illustrate how dissolution can widen certified uncertainty bands early in an event while tightening later as exsolution becomes observable, and how certified bounds can prevent both overconfident early dismissal and unnecessary shutdowns triggered by benign transients.

1. Introduction

Operational safety in drilling is governed by the interplay of uncertainty, constraints, and transients [1]. The constraint set is explicit in the form of pore-pressure and fracture-pressure limits, equipment ratings, and procedural rules. The uncertainty is pervasive, spanning formation response, mud rheology, temperature fields, slip behavior, sensor biases, and unmodeled disturbances such as heave and cuttings loading. The transients couple these elements through nonlinear dynamics, making it possible for a small disturbance to remain hidden at the surface for extended periods and then rapidly manifest as an accelerating hazard as pressure decreases and gas expands. The practical consequence is that the problem faced by monitoring systems is not only to forecast what will happen, but to determine what must be assumed plausible given what is known at a particular time. A monitoring system that provides a single predicted wellhead pressure or a single estimated kick size can be operationally fragile when the true uncertainty is large, while a system that provides conservative but uninformative bounds can be operationally unusable. Bridging this gap requires a methodology that is simultaneously physics-consistent, computationally tractable, and explicit about uncertainty in a form that supports alarm decisions [2].

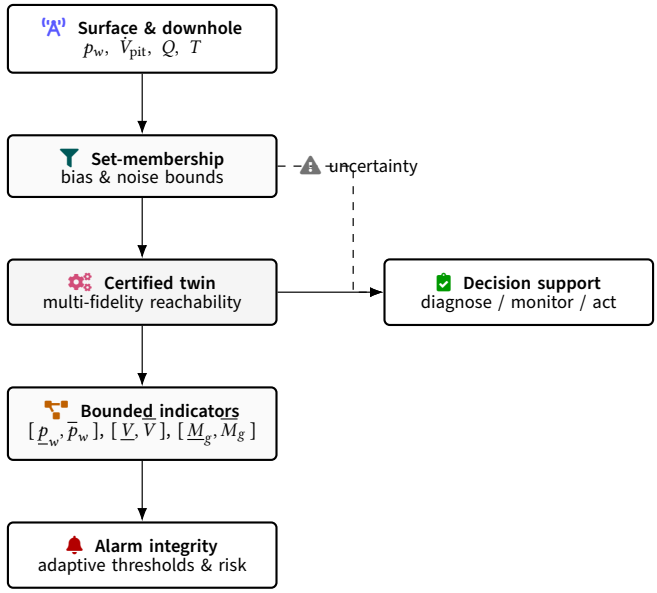


Figure 1. Certified monitoring workflow focused on alarm integrity: bounded measurements feed set-membership filtering, which constrains a multi-fidelity reachability-bounded digital twin to produce guaranteed indicator bands and time-varying integrity/risk signals for operational decisions.

Table 1. State variables in the one-dimensional annular model

Symbol	Description	Units
$p(z,t)$	Pressure along the annulus	Pa
$T(z,t)$	Mixture temperature	K
$v_m(z,t)$	Mixture superficial velocity	m/s
$\alpha(z,t)$	Free-gas volume fraction (gas holdup)	–
$c(z,t)$	Dissolved-gas mass per unit liquid mass	kg/kg
$\rho_m(z,t)$	Mixture density = $\alpha\rho_g + (1-\alpha)\rho_l$	kg/m^3
$h_m(z,t)$	Mixture specific enthalpy	J/kg

A central difficulty is that many safety-critical indicators are not directly measured where the physics is initiated. Influx occurs downhole, while measurements are taken at the surface, and the mapping between the two is mediated by multiphase transport. Even in nominally simple geometries, slip and compressibility can decouple gas migration from liquid circulation, and thermal gradients can shift densities and solubility. In synthetic or oil-based muds, dissolution introduces a further delay mechanism: a large fraction of methane mass can be stored in the liquid phase at high pressure, depressing free-gas holdup and thereby weakening early pressure and pit-gain signatures. This mechanism is not merely a subtle correction because it changes the time scale on which surface observables become informative, creating an early regime where the system is intrinsically less observable and a later regime where exsolution and expansion can become highly nonlinear. Monitoring logic that assumes an insoluble gas model can therefore be simultaneously overconfident early, by treating muted signals as evidence of no hazard, and overly reactive late, by misattributing rapid surface changes to large instantaneous influx rather than delayed release [3].

Digital twins are increasingly proposed as a remedy because they encode mechanistic constraints

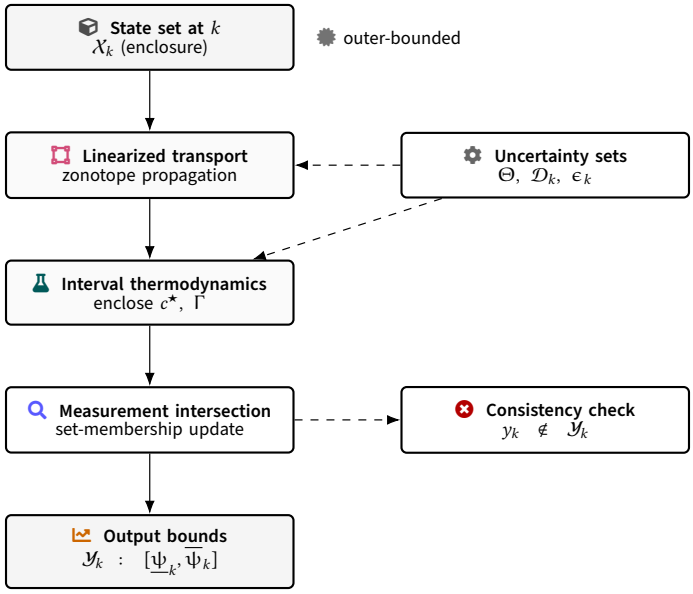


Figure 2. Reachability-bounded propagation loop: high-dimensional transport uncertainty is advanced via efficient set propagation, stiff dissolution/exsolution terms are enclosed by intervals, and measurements shrink the set only to the extent justified by bounded sensor errors, yielding certified output bands and explicit model-consistency flags.

Table 2. Gas inventories and interphase mass-transfer quantities

Symbol	Description	Representative expression	Units
m_f	Free-gas mass per unit length	$m_f = A\alpha\rho_g(p,T)$	kg/m
m_d	Dissolved-gas mass per unit length	$m_d = A(1-\alpha)\rho_l c$	kg/m
Γ	Interphase mass-transfer rate	$\Gamma = k_m a_i(c^\star - c)$	kg/(m^{3}s)
$c^\star$	Equilibrium dissolved concentration	$\Psi(p,T,c^\star;\chi) = 0$	kg/kg
a_i	Interfacial area density	$a_i = 6\alpha/d_b(\alpha,p,T;\nu)$	m^2/m^3
s_g	Formation gas source term	Boundary influx at $z = L$	kg/(m^{2}s)

and can fuse sensor streams. However, many digital twin deployments still deliver deterministic trajectories. Deterministic outputs are appealing operationally, but they implicitly place the burden of uncertainty handling on ad hoc margins and heuristics, which are difficult to justify and can become inconsistent across operating regimes. A more rigorous approach is to make the digital twin produce certified outer bounds on the quantities that drive decisions, such that, under a stated set of uncertainty assumptions, the true system behavior is guaranteed to lie within those bounds. This changes the monitoring question from predicting a single trajectory to maintaining a continuously updated set of plausible trajectories. Alarm decisions can then be posed in terms of integrity, such as whether the certified bound crosses a safety threshold, or whether the certified set is sufficiently narrow to justify particular operational actions.

A reachability-bounded digital twin is not a generic set-propagation exercise [4]. In drilling applications, the system is high-dimensional when described as a distributed annular model, it is stiff because of gas compressibility and thermodynamic partitioning, and it is subject to time-varying operational inputs and geometry. Moreover, the uncertainty set is not purely additive; it enters

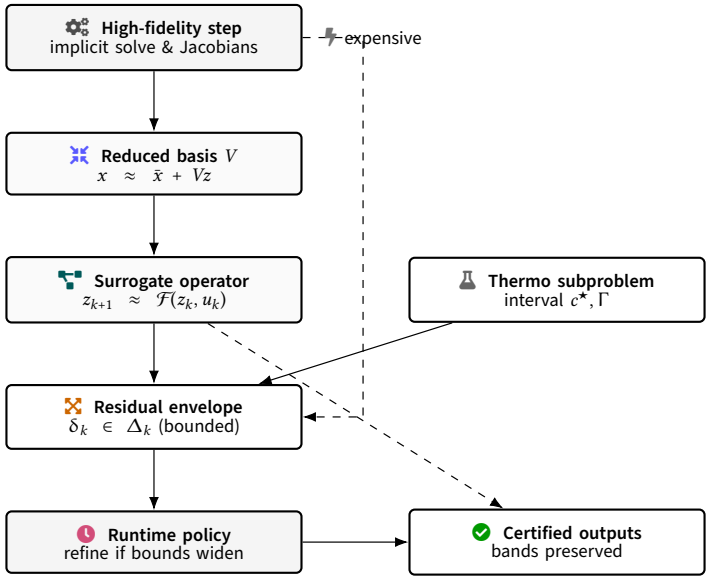


Figure 3. Multi-fidelity certification pattern: transport dynamics are accelerated via a reduced surrogate in a basis aligned with alarm-relevant modes, while a bounded residual envelope and interval-enclosed thermodynamics ensure that speedups never replace guarantees with overconfidence.

through poorly known closures and parameters, and through disturbances such as influx that act at boundaries. The challenge is therefore to define an uncertainty model that is meaningful and defensible, to propagate it in a way that yields guaranteed enclosures without explosion of conservatism, and to do so in real time. This paper addresses these issues with a multi-fidelity design that assigns certification tasks to methods that are strong where needed and cheap where possible. Stiff thermodynamic components are handled by interval enclosures that provide strong guarantees even under strong nonlinearity, while transport and hydraulics are accelerated by reduced-order surrogates whose errors are bounded and incorporated into the reachability computation.

The paper's technical thesis is that alarm integrity can be formulated and improved as a certified reachability problem [5]. Alarm integrity here refers to the ability of an alarm system to maintain a bounded probability of false alarm and missed detection under modeled uncertainty, without relying on retrospective tuning. A certified bound on indicator trajectories enables a disciplined interpretation: when the upper bound of pit gain remains below a procedural threshold, one can state that, given current uncertainty assumptions, the threshold will not be violated over a certain horizon. Conversely, when the lower bound crosses a threshold, one can state that violation is unavoidable unless operational inputs change. Intermediate cases, where the bound straddles the threshold, reveal that the uncertainty is too large to decide deterministically and that either more information must be gathered or a conservative action must be taken.

The present work is motivated by the observation that transient multiphase kick models, while steadily improving, remain constrained by dimensional simplifications and closure validity across regimes, and that improving detection is as much about making uncertainty explicit as it is about refining deterministic predictions. A review of early gas kick detection approaches emphasizes that the transient models most prominently studied are one-dimensional and incorporate only limited heat transfer and solubility, while also noting the need for broader operating-condition validity and more sophisticated modeling directions [6]. The approach in this paper complements that perspective by focusing on certification and decision support: rather than requiring a perfect model, it seeks

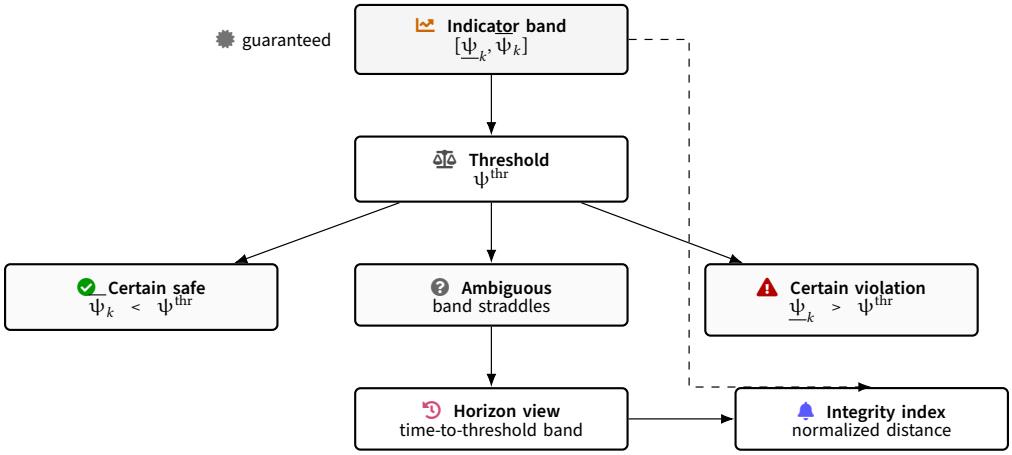


Figure 4. Alarm integrity from certified bounds: decisions are stated as set-theoretic regimes (certain safe, ambiguous, certain violation) and extended to a forecast horizon via reachability-bounded time-to-threshold bands and integrity indices that remain meaningful without assuming perfect calibration.

Table 3. Model parameters grouped by physical mechanism and uncertainty treatment

Group	Parameters	Physical role	Uncertainty representation
Slip	η, σ_v, n_h	Drift-flux velocity V_d and holdup hindrance	Bounded set for migration speed
Hydraulics	ξ, f_{eff}, μ_{eff}	Wall shear and effective viscosity	Bounded friction and rheology scaling
Thermal	κ	Wall heat-transfer coefficient	Interval on exchange strength
Solubility	χ	Equilibrium map $c^\star(p, T; \chi)$	Bounded solubility capacity and slope
Kinetics	k_m, ν	Mass-transfer rate and bubble diameter	Bounds on relaxation time scale
Sensors	Bias states, noise levels	Pit-volume and pressure measurement errors	Bounded bias with slow drift

to bound the consequences of imperfection in a way that directly supports operational alarms.

The remainder of the paper is organized as follows [7]. A physics-consistent annular model with explicit dissolved-gas inventory is formulated in a form suitable for set propagation. Uncertainty is then modeled as bounded sets over influx, closures, and sensor biases, and a reachability method is derived that yields certified enclosures of pressure, holdup, and surface indicators. A multi-fidelity acceleration strategy is introduced to reduce runtime while preserving certification by bounding surrogate residuals. The bound trajectories are finally mapped into alarm integrity metrics and decision-theoretic risk signals that can be integrated with existing well control practices. Computational experiments illustrate how the certified bounds evolve under circulation changes and under soluble versus weakly soluble conditions, highlighting the operational value of certification in both early ambiguous phases and late rapidly evolving phases.

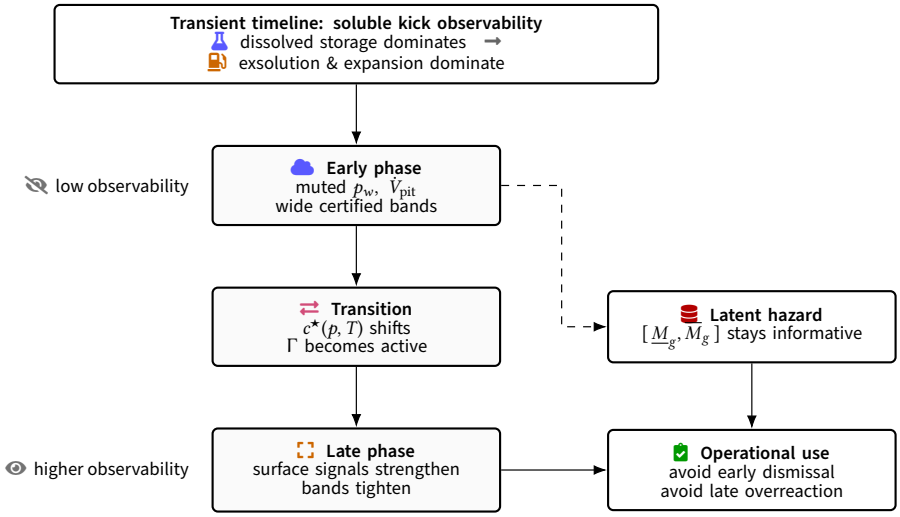


Figure 5. Qualitative evolution of certified uncertainty under soluble gas-kick transients: early dissolved storage can keep surface indicators weak while the latent total-gas band remains elevated, followed by a regime where exsolution/expansion strengthens observability and allows measurement intersections and physics constraints to tighten certified bounds.

Table 4. Uncertainty sources and associated sets in the certified digital twin

Source	Description	Set notation and remarks
Influx d_k	Gas mass inflow at $z = L$ with uncertain rate and onset time	$d_k \in \mathcal{D}_k$: time-varying compact set
Parameters θ	Slip, friction, thermal and solubility parameters	$\theta \in \Theta$: static but possibly large box
Sensor bias	Slowly varying offsets in pit and pressure readings	Bias states constrained in bounded intervals
Measurement noise	High-frequency noise and quantization	Bounded error ball around y_k
Model discrepancy	Residual between full model and surrogate dynamics	Bounded residual set $\mathcal{R}_k$, Δ_k

2. Physics-Consistent Annular Dynamics with Dissolved-Gas Inventory

The digital twin is built around a one-dimensional representation of annular flow because the dominant monitoring signals and many operational controls can be related to axial pressure and volumetric balance [8]. The purpose of the model is not to resolve all flow regimes in detail, but to maintain mechanistic constraints that prevent physically impossible interpretations and to provide a consistent mapping from downhole disturbances to surface indicators. The model must also be smooth enough to support both numerical integration and set-based propagation without requiring discontinuous regime switching. To meet these requirements, the dynamics are formulated as a constrained system with explicit inventories of free and dissolved gas, a drift-flux representation of slip, and a thermodynamic partitioning closure that can be treated implicitly.

Let $z \in [0, L]$ denote measured depth along the annulus, with $z = 0$ at the wellhead and $z = L$ at the bottom boundary of the modeled domain. The annular cross-sectional area is $A(z)$, the hydraulic diameter is $D_h(z)$, and the inclination is $\theta(z)$. The mixture consists of a liquid drilling fluid and a gas phase [9]. Gas can be present as free gas with local volume fraction $\alpha(z, t)$ and density $\rho_g(p, T)$, and as

Table 5. Structure of the reachability-bounded propagation pipeline

Stage	Operation	Output set
Initialization	Encode prior state and parameter uncertainty	$\mathcal{X}_0 \subset \mathbb{R}^n$
One-step prediction	Propagate $\mathcal{X}_k$ through F with hybrid zonotope/interval enclosures	$\widehat{\mathcal{X}}_{k+1}$
Measurement update	Intersect with measurement-consistent states via set-membership filter	$\mathcal{X}^+_{k+1}$
Indicator mapping	Evaluate bounds of alarm indicators over $\mathcal{X}^+_{k+1}$	$[\underline{\psi}_{k+1}, \overline{\psi}_{k+1}]$
Forecast horizon	Repeat over $k+1, \ldots, k+h$ for time-to-threshold bands	$\{\mathcal{X}_{k+j}\}_{j=1}^{h}$

Table 6. Multi-fidelity decomposition of the certified digital twin

Subsystem	Numerical treatment	Certification role	Cost level
Transport dynamics	Reduced-order surrogate in coordinates z_k with bounded residual	Fast propagation of distributed state	Low
Thermodynamic partitioning	Interval evaluation of $c^\star$ and Γ at each step	Guarantees across stiff nonlinearities	Moderate
Nominal trajectory	Full-order implicit integration for $\bar{x}_k$ and linearizations A_k	Reference for reduced model and residuals	High (sparse in time)
Surrogate residuals	Sigma-point evaluation and Lipschitz-based inflation	Ensures surrogate errors enter as bounded sets	Low–moderate
Refinement policy	Temporary increase in resolution or basis dimension	Tightens bounds near critical thresholds	Adaptive

dissolved gas characterized by a concentration $c(z,t)$ defined as mass of dissolved gas per unit mass of liquid. The liquid density $\rho_l(p,T,c)$ is allowed to depend on pressure and temperature through compressibility and thermal expansion, and on c through swelling. The state variables are pressure $p(z,t)$, mixture superficial velocity $v_m(z,t)$, temperature $T(z,t)$, holdup $\alpha(z,t)$, and concentration $c(z,t)$.

The mixture density is $\rho_m = \alpha\rho_g + (1-\alpha)\rho_l$. Mixture mass conservation is written in conservative form as

$$\frac{\partial}{\partial t}(A\rho_m) + \frac{\partial}{\partial z}(A\rho_m v_m) = 0. \tag{1}$$

This equation expresses that total mass per unit length changes only through axial fluxes. The modeling of gas behavior requires separate tracking of the gas mass that is free and the gas mass that is dissolved [10]. Define free-gas mass per unit length as $m_f = A\alpha\rho_g$ and dissolved-gas mass per unit length as $m_d = A(1-\alpha)\rho_l c$. Interphase mass transfer $\Gamma(z,t)$ moves gas mass between these inventories without changing total mass. The free-gas mass balance is

$$\frac{\partial}{\partial t}\left(A\alpha\rho_g\right) + \frac{\partial}{\partial z}\left(A\alpha\rho_g v_g\right) = -A\Gamma + As_g, \tag{2}$$

and the dissolved-gas balance is

$$\frac{\partial}{\partial t}\left(A(1-\alpha)\rho_l c\right) + \frac{\partial}{\partial z}\left(A(1-\alpha)\rho_l c\, v_l\right) = A\Gamma. \tag{3}$$

Table 7. Alarm indicators considered in the certified monitoring framework

Indicator	Physical meaning	Symbol	Typical threshold type
Wellhead pressure	Pressure at $z = 0$ including choke/manifold effects	$p_w(t)$	Absolute or rate-of-change limit
Pit-volume change	Cumulative imbalance between inflow and outflow	$V_{\mathrm{pit}}(t)$	Total gain/loss and gain rate
Estimated bottomhole pressure	Pressure at annulus bottom boundary	$p_{\mathrm{bh}}(t)$	Margins to pore and fracture limits
Total gas inventory	Free plus dissolved gas mass in annulus	$M_g(t)$	Latent hazard band, no fixed threshold
Consistency residual	Deviation of measured outputs from predicted set	–	Twin integrity tolerance

Table 8. Integrity metrics and temporal risk descriptors

Metric	Definition (conceptual)	Interpretation
Instantaneous integrity index	$\mathcal{I}_k = \dfrac{\Psi^{\mathrm{thr}} - \underline{\Psi}_k}{\overline{\Psi}_k - \underline{\Psi}_k + \epsilon}$	< 0: certain violation; > 1: certain non-violation; in between: ambiguous
Time-to-threshold lower bound	$\underline{\tau} = \inf\{t : \underline{\Psi}(t) > \Psi^{\mathrm{thr}}\}$	Earliest certified violation time across plausible trajectories
Time-to-threshold upper bound	$\overline{\tau} = \inf\{t : \overline{\Psi}(t) > \Psi^{\mathrm{thr}}\}$	Latest time by which violation may occur under uncertainty
Latent hazard band	Bounds on $M_g(t)$ over $\mathcal{X}_k^+$	Separable view of subsurface gas risk vs. surface indicators
Twin integrity flag	Check whether $y_k \in \mathcal{Y}_k$	Distinguishes model invalidation from kick-related alarms

The source term s_g represents gas entering from formation, which is typically applied as a boundary influx at $z = L$ rather than as a distributed source. The transport velocities v_g and v_l must reflect slip [11]. A drift-flux representation relates them to mixture velocity through a drift term V_d:

$$v_g = v_m + V_d(\alpha, p, T, v_m; \eta), \qquad v_l = v_m - \frac{\alpha}{1-\alpha} V_d(\alpha, p, T, v_m; \eta). \tag{4}$$

The parameter vector η is a compact representation of uncertain slip behavior due to bubble size distributions, annular geometry, and turbulence. The functional form of V_d is selected to be smooth and bounded. A representative choice that captures buoyancy-driven rise with hindrance is

$$V_d = \sigma_v \, H(\alpha) \sqrt{g D_h \cos\theta} \, \Phi(p, T, v_m), \qquad H(\alpha) = (1-\alpha)^{n_h}, \tag{5}$$

where σ_v is a scaling factor, n_h is a hindrance exponent, and Φ is a smooth modifier that can encode dependence on mixture velocity and effective viscosity. The point of this closure is not to claim universality, but to provide a low-parameter knob that captures how slip changes the timing of gas arrival and hence the evolution of surface indicators.

Momentum is modeled at the mixture level to keep the system compact and to avoid introducing additional stiff dynamics that are difficult to constrain with surface measurements [12]. The mixture

Table 9. Representative computational experiment scenarios

Scenario	Key features	Main qualitative outcome
Early weakly soluble kick	Low solubility, small bounded influx under circulation	Rapid rise in free-gas holdup and tightening of surface indicator bands
Early highly soluble kick	High solubility, same influx bounds	Latent gas band grows while pit and pressure bands remain narrow and ambiguous
Circulation ramp-up	Pump rate increase during ongoing event	Accelerated migration, earlier exsolution and narrowing of hazard bands
Benign hydraulic transient	Pump start/stop, friction and thermal drift only	Surface pressure transient explained within non-gas uncertainty; low gas hazard band
Surrogate stress test	Rapid exsolution and strong nonlinearity	Residual bounds inflate, triggering temporary refinement to maintain certification

momentum balance can be written as

$$\frac{\partial}{\partial t}\left(A\rho_m v_m\right) + \frac{\partial}{\partial z}\left(A\rho_m v_m^2\right) + A\frac{\partial p}{\partial z} = -A\rho_m g\cos\theta - A\Delta_w, \tag{6}$$

where Δ_w is the wall shear term expressed per unit volume. In annular drilling hydraulics, wall shear depends on rheology, cuttings, and flow regime. For the present purpose, Δ_w is expressed in a differentiable surrogate form

$$\Delta_w = \frac{2f_{\text{eff}}(\text{Re}_m, \alpha; \xi)\rho_m v_m|v_m|}{D_h}, \quad \text{Re}_m = \frac{\rho_m|v_m|D_h}{\mu_{\text{eff}}(T, \alpha; \xi)}, \tag{7}$$

where f_{eff} and μ_{eff} are smooth effective functions of a Reynolds-like number and holdup, and ξ collects uncertain rheological parameters. This form is convenient because it allows uncertainty in hydraulics to be captured through bounded sets in ξ, which can then be propagated. It is also consistent with the observation that, for alarm integrity, it is often more important to bound frictional response than to select a single friction correlation [13].

Thermal coupling enters through its effect on densities, viscosity, and solubility. A reduced energy balance is used in which a single mixture temperature is advected and exchanges heat with the surroundings. Let $h_m(\alpha, p, T, c)$ denote mixture specific enthalpy. Then

$$\frac{\partial}{\partial t}\left(A\rho_m h_m\right) + \frac{\partial}{\partial z}\left(A\rho_m v_m h_m\right) = -Av_m\frac{\partial p}{\partial z} + Aq_{\text{wall}}(T, T_f; \kappa), \tag{8}$$

where $T_f(z)$ is an ambient profile and q_{wall} is modeled as a smooth Newtonian exchange with coefficient κ. The primary role of this equation in the certified digital twin is to prevent implausible temperature trajectories and to capture the coupling between circulation changes and solubility capacity, which is strongly temperature dependent.

The key mechanism differentiating soluble and weakly soluble behavior is the relationship between local equilibrium dissolved concentration $c^\star$ and the actual concentration c. To keep the closure general while supporting certification, $c^\star$ is defined by an implicit monotone equilibrium condition [14]

$$\Psi(p, T, c^\star; \chi) = 0, \quad \frac{\partial \Psi}{\partial c^\star} > 0, \tag{9}$$

where χ is a parameter vector representing effective solubility behavior of the drilling fluid. This representation allows one to embed a thermodynamic model without committing to a specific empirical correlation in the paper's formalism. Interphase mass transfer is modeled as relaxation toward equilibrium with an interfacial area term:

$$\Gamma = k_m a_i \left(c^\star(p, T; \chi) - c\right), \quad a_i = \frac{6\alpha}{d_b(\alpha, p, T; \nu)}, \tag{10}$$

where k_m is a mass transfer coefficient, a_i is interfacial area density, and d_b is an effective bubble diameter parameterized by ν. This closure yields smooth dissolution when $c < c^\star$ and smooth exsolution when $c > c^\star$. It also introduces stiffness when $k_m a_i$ is large, which is addressed later in the multi-fidelity propagation method.

The choice to treat solubility explicitly is motivated by established modeling evidence that it materially affects ascent times and surface indicators [15]. State-of-the-art semi-analytical annular kick modeling that incorporates methane solubility in oil-based drilling fluids and shows that solubility can delay the appearance of gas at the wellhead relative to insoluble assumptions, while also demonstrating sensitivity to drilling-fluid volume-factor correlations at high pressure and temperature, provides a concrete illustration of why dissolved inventory must be represented when evaluating alarm behavior in non-aqueous systems [16]. In the certified digital twin, this motivation translates into explicit dissolved mass states and bounded uncertainty sets over χ and k_m so that the monitoring system does not have to assume a single dissolution scenario.

Surface observables are obtained by mapping the distributed state to measurable signals. Wellhead pressure is $p(0, t)$ adjusted by choke and manifold dynamics when needed. Pit volume change is linked to the net imbalance between inflow and outflow, which depends on return flow rate and surface density, both affected by gas expansion and dissolved gas release. A simple but useful relation for pit-volume rate is

$$\dot{V}_{\text{pit}}(t) = Q_{\text{in}}(t) - Q_{\text{out}}(t) + \omega(t), \tag{11}$$

where $\omega(t)$ aggregates unmodeled tank dynamics and measurement noise [17]. The outflow Q_{out} is computed from the predicted mixture velocity at the surface and annular area, adjusted for compressibility and separator conditions. In practice, pit-volume sensing drift and quantization can dominate early signals, which motivates inclusion of bounded bias states in the uncertainty model rather than treating measurements as exact.

The distributed equations define a nonlinear dynamical system that can be discretized in space to produce a finite-dimensional model. Let $x(t) \in \mathbb{R}^n$ collect discretized values of p, T, ν_m, α, c across the mesh. Operational inputs, such as pump rate and choke setting, enter through boundary conditions and can be treated as known signals $u(t)$. The influx is treated as a disturbance $d(t)$ entering as a boundary gas mass flux at $z = L$ and potentially as a liquid influx if desired. The discrete-time form over a sampling interval Δt is written abstractly as

$$x_{k+1} = F(x_k, u_k, d_k, \theta), \quad y_k = H(x_k, u_k, \theta) + \varepsilon_k, \tag{12}$$

where θ collects uncertain parameters including η, ξ, κ, χ, k_m, ν, and ε_k is measurement noise and bias. This form is the basis for reachability and certification [18].

3. Uncertainty Modeling and Reachability-Bounded Propagation

Certification requires explicit statements about what uncertainties are being bounded. The purpose is not to capture every conceivable uncertainty, but to represent the dominant ones in a manner that

is defensible and that meaningfully bounds the indicators used for alarms. The uncertainty sources that most strongly affect early alarm behavior typically include influx magnitude and timing, slip behavior governing migration speed, frictional behavior governing pressure response to circulation, thermal exchange affecting density and solubility, and the thermodynamic and kinetic parameters governing dissolution and exsolution. Sensor biases and delays are also critical because alarms often operate on differences and derivatives that amplify low-frequency drift.

The uncertainty is represented as a set $\mathcal{U}_k$ at each time step, containing admissible disturbances d_k, admissible parameter vectors θ, and admissible measurement errors. A common approach is to assume that parameters lie in a compact set Θ and disturbances in a compact set $\mathcal{D}_k$ that can vary with time. Sensor biases are modeled as bounded states with slow evolution. The certified digital twin then computes a reachable set $\mathcal{X}_k$ of admissible states at each time step, and a reachable set $\mathcal{Y}_k$ of admissible outputs. The key property is that if the true system starts in $\mathcal{X}_0$ and its uncertainties remain in the modeled sets, then $x_k \in \mathcal{X}_k$ and $y_k \in \mathcal{Y}_k$ for all k.

Formally, consider the discrete-time system [19]

$$x_{k+1} = F(x_k, u_k, d_k, \theta), \quad d_k \in \mathcal{D}_k, \quad \theta \in \Theta. \tag{13}$$

Given a set $\mathcal{X}_k$ of possible states at time k, the one-step reachable set is

$$\mathcal{X}_{k+1} = \{F(x, u_k, d, \theta) \ : \ x \in \mathcal{X}_k, \ d \in \mathcal{D}_k, \ \theta \in \Theta\}. \tag{14}$$

Exact computation of $\mathcal{X}_{k+1}$ is intractable for high-dimensional nonlinear systems, so outer approximations are computed. The paper's approach is to compute an enclosure $\widehat{\mathcal{X}}_{k+1}$ such that $\mathcal{X}_{k+1} \subseteq \widehat{\mathcal{X}}_{k+1}$, and to do so in a way that is tight enough to be operationally useful.

A central issue is conservatism growth. Naive interval arithmetic applied directly to F can lead to rapid overestimation because it ignores dependencies among variables and because repeated propagation amplifies wrapping effects. To control conservatism, the approach uses a structure-exploiting reachability method. The model is decomposed into components that are monotone or nearly monotone with respect to uncertainties, components that are stiff but low-dimensional, and components that are high-dimensional but smoother. The decomposition allows different enclosure strategies to be applied in different parts of the dynamics.

A useful starting point is to represent the reachable set as a zonotope or polytope in a reduced coordinate space where dependencies are captured [20]. However, purely polyhedral methods can be expensive at high dimension. The present method therefore uses a hybrid representation. The high-dimensional transport state is represented in a reduced basis, producing a low-dimensional coordinate vector z_k such that $x_k \approx x_k^{\mathrm{nom}} + Vz_k$, where V is a basis matrix and x_k^{nom} is a nominal trajectory computed from a point parameter estimate. The reduced dynamics are then enclosed by a combination of linearized reachability and bounded residual terms. The stiff thermodynamic variables related to dissolution are enclosed by interval methods that maintain guarantees through nonlinearity.

The reduced-order enclosure begins with a local linearization of the dynamics around the nominal trajectory:

$$x_{k+1} \approx F(\bar{x}_k, u_k, \bar{d}_k, \bar{\theta}) + A_k(x_k - \bar{x}_k) + B_k(d_k - \bar{d}_k) + G_k(\theta - \bar{\theta}) + r_k, \tag{15}$$

where A_k is the Jacobian with respect to state, B_k with respect to disturbance, G_k with respect to parameters, and r_k is a residual capturing higher-order terms. In a certified setting, r_k cannot be neglected; it must be bounded [21]. The residual bound can be obtained by Lipschitz constants of the Jacobian over the set of interest or by interval evaluation of second derivatives. While such bounds

can be conservative, they can be made practical by limiting the horizon over which linearization is used and by re-centering frequently, which is natural in a receding-horizon monitoring context.

Let $\Delta x_k = x_k - \bar{x}_k$ denote deviation from nominal. If Δx_k lies in a set $\mathcal{E}_k$ and disturbances and parameters lie in known sets, then one obtains an enclosure

$$\Delta x_{k+1} \in A_k \mathcal{E}_k \oplus B_k \Delta \mathcal{D}_k \oplus G_k \Delta\Theta \oplus \mathcal{R}_k, \tag{16}$$

where $\oplus$ denotes Minkowski sum, $\Delta\mathcal{D}_k$ and $\Delta\Theta$ are deviation sets from nominal, and $\mathcal{R}_k$ is a set containing residuals r_k. If $\mathcal{E}_k$ is chosen as a zonotope, then the linear mapping and Minkowski sums are computationally efficient, and the enclosure can be propagated with manageable cost. The challenge then becomes computing a realistic residual set $\mathcal{R}_k$. The method uses a componentwise bound derived from interval evaluation of F over the current enclosure:

$$\mathcal{R}_k \subseteq \left[\underline{F} - \bar{F} - A_k(\underline{x} - \bar{x}) - B_k(\underline{d} - \bar{d}) - G_k(\underline{\theta} - \bar{\theta}),\ \overline{F} - \bar{F} - A_k(\overline{x} - \bar{x}) - B_k(\overline{d} - \bar{d}) - G_k(\overline{\theta} - \bar{\theta}) \right], \tag{17}$$

where $\underline{\cdot}$ and $\overline{\cdot}$ denote componentwise bounds of the relevant sets. This bound exploits the fact that interval evaluation is used only on the residual, not on the entire propagation, thereby reducing dependency explosion. The bound is conservative but can be tightened by subdividing the enclosure when needed, a strategy applied adaptively when alarm-relevant outputs become too uncertain.

The stiffness introduced by dissolution kinetics and equilibrium constraints requires additional care [22]. The term $\Gamma = k_m a_i (c^\star - c)$ can change rapidly when α changes or when pressure crosses equilibrium conditions. Direct linearization can yield unstable enclosures if not handled carefully. The certified twin handles this by isolating the thermodynamic subproblem that computes $c^\star$ and Γ from (p, T, α, c) and enclosing it with interval methods at each step. In effect, at each time step, the twin computes an interval enclosure for $c^\star$ given intervals for p and T, then computes an interval enclosure for Γ given intervals for (α, c) and for uncertain parameters (k_m, χ, ν). This yields a certified enclosure for the mass-transfer source term that is then injected into the transport propagation. Because this subproblem is low-dimensional and local, the interval computations are cheap relative to full state propagation, yet they provide strong guarantees across nonlinearities.

The uncertainty sets themselves are updated as data arrive [23]. A key feature of a certified monitoring twin is that measurements should reduce uncertainty, but only to the extent justified by sensor characteristics. Measurements are incorporated through set-membership filtering. Given a predicted reachable set $\widehat{\mathcal{X}}_k$ and an observation y_k with bounded error, the updated state set is the intersection of $\widehat{\mathcal{X}}_k$ with the set of states consistent with the measurement:

$$\mathcal{X}_k^+ = \widehat{\mathcal{X}}_k \cap \{x : |0 y_k - H(x, u_k, \theta)|0 \le \epsilon_k,\ \theta \in \Theta\}. \tag{18}$$

This intersection is difficult for nonlinear H, but outer approximations can be computed by linearizing H over the set and intersecting with half-spaces. The important point is that the filter does not claim more precision than warranted; if measurement uncertainty is large or bias bounds are wide, the intersection will not shrink the set much. Conversely, when multiple sensors provide consistent constraints, the set can shrink significantly, tightening alarm bounds.

Alarm indicators are functions of state, such as wellhead pressure, pit gain, and estimated bottomhole pressure [24]. For any indicator $\psi(x)$, certification requires computing bounds

$$\underline{\psi}_k = \inf_{x \in \mathcal{X}_k^+} \psi(x), \quad \overline{\psi}_k = \sup_{x \in \mathcal{X}_k^+} \psi(x). \tag{19}$$

In practice, exact extrema are hard, so conservative bounds are computed using interval evaluation or by optimizing over zonotope enclosures with linear or convex relaxations. These bounds define the certified indicator band used for alarm logic. When the band is narrow, alarms can be made decisive. When the band is wide, the twin reports ambiguity explicitly, enabling the operational system to choose between conservative action and information gathering.

One of the most operationally relevant consequences of dissolution is that it can widen certified bands early in time [25]. Early in an event, if gas is largely dissolved, then a wide range of influx scenarios can remain consistent with near-normal pit gain and wellhead pressure. The certified twin captures this by producing wide upper bounds on possible dissolved inventory and delayed free-gas emergence. As pressure decreases in upper sections, the equilibrium condition shifts, and exsolution can become inevitable for many scenarios, reducing ambiguity. This leads to narrowing of the certified band later, not because the twin becomes more accurate, but because the physics becomes more constraining given the same uncertainty assumptions. This dynamic tightening of uncertainty is central to the integrity logic developed later.

4. Multi-Fidelity Acceleration with Bounded Surrogate Residuals

Certified reachability for distributed multiphase flow can be computationally heavy if done at full resolution and with conservative set representations. Field deployment demands a design that delivers certified bounds within operational sampling times, which can be on the order of seconds to minutes depending on the monitoring architecture [26]. The multi-fidelity strategy in this paper is to reserve expensive certified computations for components where nonlinearity and stiffness make them essential, and to accelerate the remainder using reduced-order surrogates whose errors are bounded and explicitly incorporated into the certification. This differs from purely data-driven surrogates that provide speed but not guarantees; here the surrogate is treated as an approximate operator with a certified residual envelope.

The baseline high-fidelity model is the spatially discretized annular system with n states. A nominal trajectory $\bar{x}_k$ is computed using a standard implicit integrator, producing a point prediction. Around this trajectory, local linearizations A_k are computed and used for zonotope propagation as described earlier. The multi-fidelity improvement is to replace repeated expensive evaluation of Jacobians and transport fluxes with a reduced-order operator that approximates the mapping from reduced coordinates to outputs and to key internal terms, while maintaining a bound on approximation error.

The reduction begins by constructing a basis $V \in \mathbb{R}^{n\times r}$, with $r \ll n$, that captures the dominant variation of the state relevant to alarm indicators. The basis is obtained from snapshots of the nominal model under representative transients, including pump rate changes, choke adjustments, and small gas influx scenarios [27]. The reduced coordinate is $z_k = V^{\mathsf{T}} W(x_k - \bar{x}_k)$, where W is a weighting matrix that emphasizes pressure and holdup components near the surface and in regions where solubility transitions are likely to occur. The reduced dynamics are written as

$$z_{k+1} = \mathcal{F}(z_k, u_k) + \delta_k, \tag{20}$$

where $\mathcal{F}$ is a learned or approximated reduced operator and δ_k is the residual capturing projection error, neglected modes, and parameter uncertainty effects not explicitly represented. Certification requires bounding δ_k in a set Δ_k such that $\delta_k \in \Delta_k$ for all admissible states in the current enclosure. The key to practicality is that Δ_k can be computed cheaply online, or precomputed as a function of operating point, without requiring evaluation of the full model.

The reduced operator $\mathcal{F}$ is constructed from local linearizations and from a Koopman-inspired lifting that captures weak nonlinearities. Specifically, $\mathcal{F}$ is expressed as an affine map in an augmented

feature space $\phi(z)$:

$$z_{k+1} \approx M(u_k)\,\phi(z_k) + b(u_k), \tag{21}$$

where $\phi(z)$ includes z and a small number of quadratic cross terms selected to capture compressibility-driven nonlinearities and holdup-pressure coupling. The matrices $M(u)$ and $b(u)$ are fitted online from a small set of recent linearizations, ensuring that the surrogate tracks slow parameter drift. This approach is chosen because it preserves interpretability and supports residual bounding: the difference between the high-fidelity step and the surrogate step can be evaluated at a few representative points within the current enclosure to bound the residual, and the bound can be inflated conservatively when the enclosure is large.

Bounding δ_k is the critical certification step [28]. The method uses a two-layer bound. First, a structural bound is derived from projection error. Let $P = VV^{\mathsf{T}}W$ denote the projection operator. The one-step high-fidelity deviation is $\Delta x_{k+1} = F(\bar{x}_k + Vz_k, u_k, d_k, \theta) - \bar{x}_{k+1}$. The reduced prediction corresponds to Vz_{k+1}^{pred} with $z_{k+1}^{\text{pred}} = \mathcal{F}(z_k, u_k)$. The residual in state space is

$$e_{k+1} = \Delta x_{k+1} - Vz_{k+1}^{\text{pred}}. \tag{22}$$

A bound on e_{k+1} can be obtained by bounding the component orthogonal to the basis and the surrogate mismatch within the basis. The orthogonal component can be bounded by the energy of neglected singular values from the snapshot matrix, inflated to account for uncertainty. The in-basis component can be bounded by evaluating the surrogate mismatch at a small number of sigma points within the current reduced enclosure. The resulting state-space residual set is then mapped into reduced space as $\Delta_k = V^{\mathsf{T}}W\mathcal{E}_{k+1}$, yielding a certified bound on δ_k.

Second, to ensure robustness to nonlinearity, the bound is augmented by a Lipschitz-based term proportional to the diameter of the current enclosure [29]. If the reduced enclosure for z_k is a zonotope with generators G_k, then a conservative diameter measure is $|0G_k|0_1$. The bound is inflated as

$$\Delta_k \leftarrow \Delta_k \oplus \{\delta : |0\delta|0_\infty \le \lambda_\delta |0G_k|0_1\}, \tag{23}$$

where λ_δ is a calibrated constant representing worst-case curvature not captured by the surrogate. This inflation ensures certification even when the surrogate was trained on a narrower region than the current enclosure, at the cost of added conservatism that is automatically reduced as the enclosure tightens through measurement intersections.

The thermodynamic subproblem for $c^\star$ and Γ is not approximated by the surrogate in a purely data-driven manner because it is stiff and because its nonlinearity is a primary driver of alarm behavior. Instead, the subproblem is evaluated using interval enclosures at each step, as described previously, and the resulting interval for Γ is fed into the reduced transport model as a bounded input [30]. This hybrid strategy yields a favorable division of labor: expensive but low-dimensional interval computations provide strong guarantees where needed, while the large transport state is propagated cheaply in reduced space with bounded residuals.

The multi-fidelity architecture also supports dynamic refinement. When an alarm-relevant indicator band becomes too wide, the twin can refine by temporarily increasing the reduced dimension r or by performing a limited number of high-fidelity evaluations to tighten residual bounds. This refinement is not described as a procedural list but as a policy: the twin monitors the width of certified bounds on wellhead pressure and pit gain and allocates computational resources when those widths exceed operational tolerance. Conversely, when the system is quiescent and bounds are narrow, the twin relies primarily on the surrogate, reducing runtime without sacrificing certification.

The value of bounded surrogates in this setting is that they decouple certification from perfect modeling. A surrogate that is imperfect but bounded is preferable to a high-fidelity model that is too slow to be used consistently [31]. In addition, the residual bounding formalism provides a transparent audit trail: any time the twin tightens or widens an alarm band, it can attribute the change to either physical uncertainty, measurement inconsistency, or surrogate residual inflation. This interpretability supports operational trust and enables targeted improvements, such as reducing sensor bias bounds or refining solubility parameter bounds, rather than blindly retuning alarm thresholds.

5. Alarm Integrity Metrics and Decision-Theoretic Risk Signals

Certified bounds become operationally meaningful only when mapped into alarm decisions and integrity statements. Traditional alarms in drilling often operate on thresholds applied to pit gain rate, total pit gain, wellhead pressure changes, or combinations of such signals. These alarms are typically tuned to balance false alarms against missed detections based on experience. In the presence of strong uncertainty and soluble gas behavior, fixed thresholds can behave inconsistently across regimes: they can be too sensitive when benign transients occur and too insensitive when dissolution delays observables [32]. The certified twin enables a different formulation in which the alarm system reasons about sets of plausible indicator trajectories and reports integrity metrics that quantify decision ambiguity.

Let ψ_k denote a scalar alarm indicator computed from state, such as pit gain $V_{\mathrm{pit}}(k)$ or wellhead pressure $p_w(k)$. The certified twin provides a band $[\underline{\psi}_k, \overline{\psi}_k]$. Consider a threshold ψ^{thr} associated with a procedural response. Three regimes are possible. If $\overline{\psi}_k < \psi^{\mathrm{thr}}$, then all trajectories consistent with uncertainties remain below the threshold, and the alarm should not trigger if the goal is to avoid false alarms. If $\underline{\psi}_k > \psi^{\mathrm{thr}}$, then all consistent trajectories violate the threshold, and the alarm should trigger because violation is inevitable without intervention. If the band straddles the threshold, then the alarm decision is ambiguous given the modeled uncertainty, and integrity requires reporting this ambiguity explicitly rather than forcing a binary decision based on a point estimate.

To quantify ambiguity, the twin computes an integrity index that measures the normalized distance between the threshold and the band:

$$\mathcal{I}_k = \frac{\psi^{\mathrm{thr}} - \underline{\psi}_k}{\overline{\psi}_k - \underline{\psi}_k + \epsilon}, \tag{24}$$

where ϵ is a small regularization. Values $\mathcal{I}_k < 0$ correspond to certain violation, values $\mathcal{I}_k > 1$ correspond to certain non-violation, and intermediate values quantify how much of the band lies below the threshold. This index does not assume a probability distribution; it is a set-based integrity measure. When probabilistic information is available, for example when measurement noise is modeled stochastically within bounds, the twin can map the set to a conservative probability bound using worst-case distributions, but the set-based index remains valuable because it is defensible under minimal assumptions [33].

Alarm integrity is also a temporal property. A pit gain threshold might not be violated at the current time but could be inevitably violated within a horizon given current uncertainty. The twin therefore computes reachability-bounded forecast bands over a horizon h and evaluates whether the threshold will be crossed. The result is a certified time-to-threshold band:

$$\underline{\tau} = \inf\{t \in [0, h] : \underline{\psi}(t) > \psi^{\mathrm{thr}}\}, \quad \overline{\tau} = \inf\{t \in [0, h] : \overline{\psi}(t) > \psi^{\mathrm{thr}}\}, \tag{25}$$

with the understanding that these are computed numerically from discrete-time propagation. If $\overline{\tau}$ is large, then even the worst-case plausible trajectory stays below threshold for a long time. If $\underline{\tau}$

is small, then all plausible trajectories cross quickly, demanding immediate action. If the interval is wide, the decision is time-ambiguous, and the appropriate response depends on operational risk posture [34].

The decision-theoretic layer maps integrity metrics into recommended actions without claiming to replace procedures. The actions can include maintaining operation, increasing monitoring intensity, applying a controlled diagnostic perturbation, or initiating well-control procedures. In a certified framework, the recommended action is driven by whether uncertainty is reducible and by the cost of conservative action. If the band straddles a threshold and is wide because of sensor bias uncertainty, then improving sensor calibration or using additional measurements could reduce ambiguity. If the band is wide because the physics is intrinsically unobservable early due to dissolution, then ambiguity may not be reducible quickly, and conservative action may be preferred.

A particularly important integrity concept for soluble kicks is the distinction between indicator-based certainty and hazard-based certainty [35]. Pit gain can remain small even when gas mass is accumulating dissolved. The hazard in such a case is not immediate surface pit gain but the potential for delayed free-gas release and rapid unloading at shallow depths. The certified twin therefore defines an internal hazard metric based on total gas mass in the annulus, including dissolved and free gas:

$$M_g(k) = \int_0^L A(z) \left(\alpha(z,k)\rho_g(z,k) + (1 - \alpha(z,k))\rho_l(z,k)c(z,k) \right) \, dz. \tag{26}$$

The twin computes a certified band on $M_g(k)$ and uses it as a latent hazard indicator. An alarm policy based solely on pit gain might miss a scenario where M_g is large but still dissolved. The certified twin exposes this by producing a wide or elevated band on M_g even when pit gain bands are low. This does not force an alarm, but it informs integrity by showing that non-violation of surface thresholds does not imply absence of hazard under soluble conditions [36].

This latent hazard concept aligns with mechanistic understanding that dissolution can alter the timing of surface indicators, and it is supported by state-of-the-art modeling evidence that methane dissolution in synthetic and oil-based fluids can be significant and measurable in mechanistic models. A mechanistic gas kick model for riser dynamics that predicts key indicators and explicitly models gas solubility in synthetic-based mud, including validation of methane liquid-phase mole fraction predictions with a maximum 8% deviation from a process simulator and agreement on bubble point estimates, provides an example of how dissolved inventory can be treated as a primary state rather than a secondary correction [37]. In the alarm integrity framework, this motivates defining hazard metrics that account for dissolved mass, and it motivates bounded uncertainty sets over dissolution parameters so that the twin's hazard band reflects plausible dissolution capacity rather than assuming it away.

The integrity layer must also address false alarms caused by benign transients. Pump ramping, temperature drift, and friction changes can produce wellhead pressure changes that resemble early kick signatures. In a deterministic alarm, these transients can trigger repeated false alarms, leading to alarm fatigue and operational disruption. In a certified twin, such transients are represented as bounded disturbances and parameter variations [38]. If a wellhead pressure change can be explained entirely by bounded friction variation and thermal drift, then the certified band on latent gas mass will remain low, and the integrity index relative to gas-related thresholds will reflect that the event is ambiguous or likely benign. Conversely, if explaining the observed change requires a large increase in latent gas mass within the modeled bounds, then the gas hazard band will rise. This separation is a key benefit of physics-consistent certification: it does not guarantee correct classification under all conditions, but it prevents classification that violates modeled constraints.

An additional integrity element is consistency checking. If measured signals fall outside the predicted output set $\mathcal{Y}_k$, then either uncertainties have been underestimated, sensors are faulty, or the model structure is missing an important mechanism. The twin reports this as an integrity violation of the digital twin itself, distinct from a kick alarm. This distinction matters operationally: a kick alarm is a statement about the well state, while a twin integrity violation is a statement about the monitoring system's assumptions. The appropriate response to a twin integrity violation may be to widen uncertainty bounds, switch to a fallback monitoring mode, or verify sensors, rather than to initiate well control based on an untrusted model [39].

Finally, alarm integrity must be compatible with regulatory constraints and operational practices. The certified twin does not prescribe replacing existing alarms; rather, it provides additional signals that can be layered on top of existing thresholds. For example, the twin can provide adaptive thresholds based on uncertainty width, or it can provide a confidence measure that conditions whether a procedural threshold is treated as decisive. The value of certification is that such adaptations are grounded in explicit uncertainty propagation rather than heuristic scaling.

6. Computational Experiments and Discussion

Computational experiments are used to illustrate how the certified multi-fidelity twin behaves under representative transients and how it changes alarm interpretation under soluble versus weakly soluble conditions. The purpose of these experiments is to examine the evolution of certified bands and integrity metrics, not to reproduce a particular field case in detail [40]. The model domain represents a vertical or mildly deviated annulus with depth-dependent geometry and ambient temperature profile. Operational inputs include pump rate trajectories and surface backpressure, treated as known. Disturbances include a bounded gas influx applied at the bottom boundary with uncertain rate and start time. Parameter uncertainty sets include bounded friction scaling, bounded slip scaling, bounded heat transfer coefficient, bounded solubility capacity parameters, and bounded mass transfer rate, along with bounded sensor bias in pit volume.

The first class of experiments examines early-stage behavior under circulation. A small bounded influx is initiated, with a range of possible rates consistent with uncertainty [41]. In a weakly soluble configuration, where solubility capacity is low, a significant fraction of influx appears as free gas. The certified band on holdup near the bottom increases promptly, and the band on wellhead pressure begins to widen and shift as compressibility increases. Because the relationship between influx and wellhead pressure is mediated by migration time, early wellhead pressure bands can still be wide, but the latent hazard band on total gas mass rises in a manner that is constrained by mass conservation and by free-gas transport. The pit gain band also begins to rise as gas expansion contributes to outflow imbalance. In this regime, measurement intersections can rapidly tighten uncertainty because surface observables respond relatively promptly to free gas, making the system more observable.

In a highly soluble configuration, the early response is qualitatively different. The same bounded influx produces a large increase in dissolved mass near the bottom, while free-gas holdup can remain small within the plausible set [42]. The certified band on wellhead pressure remains relatively close to baseline initially, and the pit gain band can remain near zero even while the latent hazard band on total gas mass rises. This is not a failure of the twin but a representation of physical ambiguity. The key output is that the twin's integrity index relative to pit gain thresholds remains in the ambiguous regime for longer, while the latent hazard band indicates that a significant amount of gas mass could plausibly be present. In a deterministic alarm system, the absence of pit gain would often be interpreted as absence of hazard; the certified twin explicitly prevents that inference by showing that, under modeled dissolution uncertainty, non-violation of pit gain does not exclude substantial latent gas mass.

A second class of experiments examines the effect of circulation changes. Circulation affects advection, slip behavior through turbulence, and temperature evolution [43]. Under increased pump rate, the migration of both dissolved and free gas is accelerated. In weakly soluble conditions, this can bring free gas to the surface sooner, tightening the time-to-threshold band and making alarms more decisive. In highly soluble conditions, increased circulation can transport dissolved gas upward into regions of lower pressure where equilibrium capacity decreases, potentially inducing exsolution. The certified twin captures this through the interval-enclosed equilibrium map $c^{\star}(p, T)$ and through the bounded mass transfer term Γ. As pressure decreases along the upward path, the twin's predicted enclosure for Γ can become strongly negative in upper cells, indicating that exsolution is possible or inevitable for many scenarios. This transition often causes a narrowing of the hazard band because the physics becomes more constraining: once exsolution is triggered, the relationship between gas mass and wellhead pressure becomes stronger, and measurements can eliminate more scenarios. Operationally, this means that uncertainty can tighten sharply after a regime transition, and the twin reflects this by shrinking the certified band widths [44].

A third class of experiments focuses on benign transients that often produce false alarms. Pump startup and shutdown generate pressure waves and friction changes. Thermal drift over longer times produces density changes that can bias inferred flow imbalance. In the experiments, friction scaling and heat transfer coefficients are allowed to vary within bounded sets. The twin propagates these uncertainties and produces an output band for wellhead pressure. When an observed wellhead pressure transient lies within this band, the twin's consistency check passes, and the state set is intersected but not forced to include an influx [45]. The latent hazard band on total gas mass remains low because the model can explain the observations through friction and thermal effects alone within bounds. As a result, integrity metrics conditioned on gas hazard remain in the non-violation regime. This does not eliminate all false alarms, but it creates a mechanism for distinguishing transients that are explainable by non-gas uncertainties from those that require additional gas mass to explain.

The multi-fidelity acceleration is evaluated by comparing certified bound propagation with and without surrogate usage. Without surrogates, zonotope propagation with residual interval bounding can be costly because it requires repeated Jacobian evaluations and residual computations at each step. With surrogates, the transport propagation is performed in reduced space, and the residual bounds are computed using limited high-fidelity evaluations at sigma points [46]. The experiments show that, in quiescent regimes, surrogate residual bounds remain small, and certified indicator bands are nearly identical to those produced by full propagation. During rapid regime transitions, such as exsolution onset, residual bounds increase, widening indicator bands modestly. The twin responds by temporarily allocating more high-fidelity evaluations, which tightens residual bounds and recovers tight indicator bands. The essential point is that certification is preserved throughout because residual inflation is explicitly included in the bound propagation; when the surrogate is less reliable, the twin reports wider bands rather than providing an overconfident output.

An important operational interpretation of these results is that certification naturally leads to adaptive conservatism. Early in a soluble event, bands can be wide, and the twin reports ambiguity rather than a crisp alarm. As time progresses and physics and measurements constrain the set, bands can narrow and alarms become more decisive [47]. This is consistent with the reality that early detection in soluble systems is intrinsically harder. The certified twin does not claim to make the system more observable; rather, it provides a disciplined way to represent what is and is not implied by available data and modeled uncertainty. This can be valuable for preventing premature dismissal of a hazard and for preventing unnecessary shutdowns when data are consistent with benign explanations.

The experiments also highlight the sensitivity of certification to the choice of uncertainty sets. If solubility capacity bounds are extremely wide, early hazard bands can become so wide that they provide little actionable information. If bounds are unrealistically narrow, certification becomes

meaningless because the true system may lie outside the assumed uncertainty [48]. The value of the set-based approach is that it makes this dependence explicit. Operational deployment would involve selecting uncertainty sets based on laboratory measurements, historical data, and conservative engineering judgment. Over time, the sets can be refined as more data become available. The certified twin provides feedback by reporting when measurements consistently lie near the boundary of the predicted output set, indicating that sets may need adjustment.

Finally, these experiments motivate a view of alarm systems as layered. A deterministic threshold alarm remains useful as a fast heuristic. The certified twin augments it by providing integrity metrics that qualify the alarm's reliability under current uncertainty [49]. In particular, when the deterministic alarm triggers but the certified band indicates that threshold violation is not inevitable under modeled uncertainty, the operator can interpret the alarm as potentially false and seek additional evidence. Conversely, when the deterministic alarm does not trigger but the certified hazard band is elevated, the operator can interpret the situation as potentially hazardous despite muted surface indicators. This bidirectional qualification is especially important in soluble systems.

7. Conclusion

This paper developed a certified multi-fidelity digital twin methodology for soluble gas-kick transients with the specific aim of improving alarm integrity and real-time risk quantification. The approach centers on producing guaranteed outer bounds on safety-critical indicators, rather than single deterministic trajectories, under bounded uncertainty in influx, hydraulics, thermal exchange, and thermodynamic partitioning between free and dissolved gas. A physics-consistent one-dimensional annular model was formulated with explicit inventories for free and dissolved gas, drift-flux slip representation, and smooth dissolution and exsolution closure [50]. Uncertainty was propagated through reachability-bounded methods that combine zonotope-based linearized set propagation with interval enclosures for stiff thermodynamic components, while measurements were incorporated through set-membership intersections that tighten bounds only to the extent justified by sensor error and bias assumptions.

To enable real-time deployment, a multi-fidelity acceleration strategy was introduced in which transport dynamics are propagated through reduced-order surrogates whose residual errors are bounded and incorporated into the certified enclosure, while thermodynamic solubility subproblems are handled by certified interval evaluation. The resulting digital twin produces time-varying indicator bands, integrity indices relative to operational thresholds, and latent hazard bands based on total gas inventory that remain informative when surface indicators are muted by dissolution. Computational studies demonstrated how dissolution can widen certified uncertainty early in an event and how bounds can tighten later as exsolution and expansion increase observability, providing a principled representation of ambiguity that can prevent both overconfident early dismissal and unnecessary operational interruptions.

The broader implication is that monitoring performance is limited not only by model fidelity but also by the explicit handling of uncertainty. Certification provides a transparent mechanism for mapping uncertainty into alarm decisions, and multi-fidelity design provides a pathway to make such certification computationally feasible in practice. Future extensions can incorporate richer geometry effects through bounded model discrepancy terms, integrate additional sensors through set-based fusion, and refine uncertainty sets through systematic calibration while maintaining the core requirement that the digital twin's outputs remain guaranteed enclosures under stated assumptions [51].

References

[1] Anjanava Das Purkayastha, Rohit Rana, Rahul Talreja, and Nanthakumar Rajaiah. "Drilling Event Chart: A Kick Prevention Tool". In: *SPE Gas & Oil Technology Showcase and Conference*. SPE, Oct. 21, 2019. DOI: 10.2118/198660-ms.

[2] J.E. Hofmann, D.K. Fusselman, and R.J. Liles. "New Source Air Pollution Permits in Texas and New Mexico". In: *Permian Basin Oil and Gas Recovery Conference*. SPE, Mar. 16, 1994. DOI: 10.2118/27705-ms.

[3] O.L.A. Santos, J.R.P. Mendes, and Paulo Ribeiro. "The Development and Application of a Software to Assist the Drilling Engineer During Well Control Operations in Deep and Ultra Deep Waters". In: *SPE Latin American and Caribbean Petroleum Engineering Conference*. SPE, Apr. 27, 2003. DOI: 10.2118/81184-ms.

[4] Miao He, Gonghui Liu, Jun Li, Mengbo Li, and Li. "A study of rapid increasing choke pressure method for sour gas kicks during managed pressure drilling". In: *International Journal of Oil, Gas and Coal Technology* (Dec. 23, 2015).

[5] Hermann F. Spoerker, Michael J. Jellison, and Wolfgang Havlik. "What Really Happens to High Strength Drillpipe When Taking a Sour-Gas Kick?" In: *IADC/SPE Drilling Conference* (Mar. 4, 2008). DOI: 10.2118/112678-ms.

[6] Ahmad K Sleiti, Gorakshnath Takalkar, Muftah H El-Naas, Abu Rashid Hasan, and Mohammad Azizur Rahman. "Early gas kick detection in vertical wells via transient multiphase flow modelling: A review". In: *Journal of Natural Gas Science and Engineering* 80 (2020), p. 103391.

[7] B. Hamoudi, Khelil Kartobi, Hani H. Qutob, Paco Vieira, Marc Antoine Saad, and Fabian Torres. "Drilling Hazard Mitigation Technology Enables Conventionally Undrillable Prospects To Be Drilled With Reduced Non-Productive Time And Increased Operational Safety: Application Of Solid Expandable Liners And Managed Pressure Drilling In Algeria Nezla Field". In: *North Africa Technical Conference and Exhibition*. SPE, Feb. 20, 2012. DOI: 10.2118/151000-ms.

[8] B.W. Swanson, B. Gilvary, and F. McEwan. "Experimental Measurement and Modeling of Gas Solubility in Invert Emulsion Drilling Fluids Explains Surface Observations During Kicks". In: *European Petroleum Conference* (Oct. 16, 1988). DOI: 10.2118/18371-ms.

[9] F.F. Shanks, D.S. Hammett, and H.L. Zinkgraf. "Experience Drilling in Deepwater High Current Areas". In: *Offshore Technology Conference*. OTC, Apr. 30, 1979. DOI: 10.4043/3582-ms.

[10] Harald Linga, Anja Torsvik, and Arild Saasen. "Kick Detection Capability of Oil-Based Muds in Well Control Situations". In: *SPE Bergen One Day Seminar*. SPE, Apr. 20, 2016. DOI: 10.2118/180039-ms.

[11] Emeka Emmanuel Okoro, Adewale Dosunmu, and Sunny E. Iyuke. "Data on cost analysis of drilling mud displacement during drilling operation". In: *Data in brief* 19 (May 18, 2018), pp. 535–541. DOI: 10.1016/j.dib.2018.05.075.

[12] Helio Santos, Erdem Catak, and Sandeep Valluri. "Kick Tolerance Misconceptions and Consequences to Well Design". In: *SPE/IADC Drilling Conference and Exhibition* (Mar. 1, 2011). DOI: 10.2118/140113-ms.

[13] Mate Ledenko. *Razmatranja kontrole tlaka u podvodnom bušenju*. Sept. 27, 2017.

[14] Jan Runar Tangstad. *Assessment of dynamic barriers in oil/gas well operations: Vurdering av dynamiske barrierer i olje/gass brønner*. Jan. 1, 2014.

[15] E.N. Monteiro. "Study of Methane Solubility in Organic Emulsions Applied to Drilling Fluid Formulation and Well Control". In: *SPE Annual Technical Conference and Exhibition*. SPE, Oct. 9, 2005. DOI: 10.2118/101518-stu.

[16] Kaushik Manikonda, Abu Rashid Hasan, Omer Kaldirim, Jerome J Schubert, and Mohammad Azizur Rahman. "Understanding gas kick behavior in water and oil-based drilling fluids". In: *SPE Kuwait oil and gas show and conference*. SPE. 2019, D043S023R001.

[17] Geoffrey Lee. *Coherence and defect formation in finite-temperature Bose-Einstein condensates*. Feb. 1, 2013.

[18] Sun Shihui, Yan Tie, BI Xueliang, Chen Xun, and Zhang Nan. "Retraction Notice: Wellbore Flow Analysis of a Gas-Kick Well During Shut-In". In: *The Open Fuels & Energy Science Journal* 9.1 (Dec. 30, 2016), pp. 138–138. DOI: 10.2174/1876973x01609010138.

[19] A.T. Duguid. "Use Of Magnetic Ranging Logging Tool To Direct Amoco . Steep A7-28-66-07 W6M Drilling". In: *Journal of Canadian Petroleum Technology* 22.02 (Mar. 1, 1983). DOI: 10.2118/83-02-02.

[20] Marta Volonteri. *Evolution of massive black holes*. Sept. 12, 2007.

[21] Trey Brown and L. Yu Lin. *Theoretical Thought to Practical Application*. May 11, 2001.

[22] Michael Runtuwene, Sanny Suprihono, Dany Rizka, Andi Eka Prasetia, Julmar Shaun Sadicon Toralde, and Steve William Nas. "Pressurized Mud Cap Drilling Drastically Reduces Non-Productive Time in Soka Field, South Sumatera". In: *Middle East Drilling Technology Conference & Exhibition*. SPE, Oct. 26, 2009. DOI: 10.2118/125311-ms.

[23] Aldyth Sukapradja, Roni Herdianto, Jesse Clark, Cepi M. Adam, Untung Ashari, Baginda Saragih, Rio Sitorus, and Bayu Giriansyah. "Integrated 3D Pore Pressure Characterisation and Modeling: Methodology & Application in Sisi Nubi Field, Mahakam - Indonesia". In: *SPE/IATMI Asia Pacific Oil & Gas Conference and Exhibition*. SPE, Oct. 17, 2017. DOI: 10.2118/186310-ms.

[24] Rohani M.J., Azam A.R., Lunne T., and Strout J.M. "Foundation Integrity: Shallow Gas Mitigation Using the XPP Monitoring Tool - An Offshore Malaysia Case History". In: *Offshore Technology Conference-Asia*. OTC, Mar. 25, 2014. DOI: 10.4043/24843-ms.

[25] David VonSeggern. "2005 Annual SSA Meeting Report". In: *Seismological Research Letters* 76.6 (Nov. 1, 2005), pp. 714–734. DOI: 10.1785/gssrl.76.6.714.

[26] Alcantara Santos and Otto Luiz. "Technology Focus: Well Integrity (January 2013)". In: *Journal of Petroleum Technology* 65.01 (Jan. 1, 2013), pp. 104–104. DOI: 10.2118/0113-0104-jpt.

[27] J. Promping, Apiwat Wisitsorasak, B. Chatthong, S. Sangaroon, R. Picha, and Atsushi Fukuyama. "Predictions of Plasma Behavior Due to Pellet Injection for Future Thailand Tokamak". In: *Plasma and Fusion Research* 14.0 (Oct. 9, 2019), pp. 3403154–3403154. DOI: 10.1585/pfr.14.3403154.

[28] Anthony J. Smalley, Ralph E. Harris, and Gary D. Bourn. *TECHNOLOGIES TO ENHANCE OPERATION OF THE EXISTING NATURAL GAS COMPRESSION INFRASTRUCTURE*. Jan. 1, 2003. DOI: 10.2172/819329.

[29] Jyotsna Sharma, Otto L. A. Santos, Giuseppe Feo, Oloruntoba Ogunsanwo, and Wesley Williams. "Well-scale multiphase flow characterization and validation using distributed fiber-optic sensors for gas kick monitoring." In: *Optics express* 28.26 (Dec. 9, 2020), pp. 38773–38787. DOI: 10.1364/oe.404981.

[30] W.R. Matthews. *How To handle acid gas H/sub 2/S And CO/sub 2/ Kicks*. Nov. 15, 1984.

[31] Kenneth Olsvik, Morten Hansen Jondahl, Kjell Rune Toftevåg, Remi Kippersund, Geir Elseth, and Ivar Kjøsnes. "Disruptive Clamp-On Technology Tested for Mud Measurement". In: *SPE Norway One Day Seminar*. SPE, May 13, 2019. DOI: 10.2118/195624-ms.

[32] Mostafa Mirzaee Aliabadi, Iraj Mohammadfam, and Ahmadreza ahmadi gahar. "Root causes analysis of the Blow out of oil and gas wells in the drilling industry using Bow-Tie Analysis". In: *Iran Occupational Health* 15.6 (Feb. 10, 2019), pp. 16–24.

[33] Young Wan Hong and Robert van Kuilenburg. "Active Mud Line Pumping, Design, Testing and Future Possibilities in Rig Design". In: *IADC/SPE Drilling Conference and Exhibition*. SPE, Mar. 6, 2018. DOI: 10.2118/189579-ms.

[34] Jiří Maršálek, Pavel Brož, and Marek Bobák. "Complex biogas membrane upgrading to BioCNG at agriculture biogas plant". In: *Chemical Papers* 74.12 (June 7, 2020), pp. 4227–4239. DOI: 10.1007/s11696-020-01238-7.

[35] Selim S Shaker and David J Reynolds. "Kicks and Blowouts Prediction Before and During Drilling in the Over-Pressured Sediments". In: *Offshore Technology Conference*. OTC, May 4, 2020. DOI: 10.4043/30711-ms.

[36] T. Nagashima, M. Takano, Takeshi Izumiyzma, Daisuke Barada, Shigeo Kawata, Yanjun Gu, Qing Kong, Ping Xiao Wang, Y. Y., and Wei-Min Wang. "High-Quality Ion Beam Generation in Laser Plasma Interaction". In: *Proceedings of the 12th Asia Pacific Physics Conference (APPC12)*. Vol. 2. Journal of the Physical Society of Japan, Mar. 19, 2014, pp. 015093–. DOI: 10.7566/jpscp.1.015093.

[37] Kaushik Manikonda, Abu Rashid Hasan, Abinash Barooah, Nazmul H Rahmani, Muftah El-Naas, Ahmad Khalaf Sleiti, and Mohammad Azizur Rahman. "A mechanistic gas kick model to simulate gas in a riser with water and synthetic-based drilling fluid". In: *Abu Dhabi International Petroleum Exhibition and Conference*. SPE. 2020, D012S116R009.

[38] Xiaohui Sun, Baojiang Sun, and Zhiyuan Wang. "Wellbore Dynamics of Kick Evolution Considering Hydrate Phase Transition on Gas Bubbles Surface During Deepwater Drilling". In: *Volume 8: Polar and Arctic Sciences and Technology; Petroleum Technology*. American Society of Mechanical Engineers, June 25, 2017. DOI: 10.1115/omae2017-61125.

[39] Jeff Spath. "Emerging Frontiers: Focus on East Africa". In: *Journal of Petroleum Technology* 65.10 (Oct. 1, 2013), pp. 14–16. DOI: 10.2118/1013-0014-jpt.

[40] Reza Asgharzadeh Shishavan, Casey Hubbell, Hector D. Perez, John D. Hedengren, David S. Pixton, and Anthony Paul Pink. "Multivariate Control for Managed-Pressure-Drilling Systems by Use of High-Speed Telemetry". In: *SPE Journal* 21.02 (Apr. 14, 2016), pp. 459–470. DOI: 10.2118/170962-pa.

[41] P. C. H. Veeken and Marianne Rauch-Davies. "AVO attribute analysis and seismic reservoir characterization". In: *First Break* 24.2 (Feb. 1, 2006), pp. 41–52. DOI: 10.3997/1365-2397.2006004.

[42] Harald Linga, Knut Steinar Bjorkevoll, Jan Ole Skogestad, and Arild Saasen. "Gas Influx into Drilling Fluids During Flow Check Operations as Affected by Gas Absorption Characteristics of the Drilling Fluid". In: *SPE/IADC Drilling Conference and Exhibition* (Mar. 14, 2017). DOI: 10.2118/184686-ms.

[43] Tawfik Elshehabi and Ilkin Bilgesu. "Well Integrity and Pressure Control in Unconventional Reservoirs: A Comparative Study of Marcellus and Utica Shales". In: *SPE Eastern Regional Meeting*. SPE, Sept. 13, 2016. DOI: 10.2118/184056-ms.

[44] H.R. Lima and Hans C. Juvkam-Wold. "Computational Hydraulic Analysis of a Deepwater Well Drilled With Synthetic-Based Mud in a Riserless Drilling Configuration". In: *SPE Annual Technical Conference and Exhibition* (Sept. 27, 1998). DOI: 10.2118/49057-ms.

[45] D.L. Whitman, J.F. Evers, and R.E. Terry. "Using Computer Graphics and Animation To Teach Petroleum Engineering Concepts". In: *International Meeting on Petroleum Engineering*. SPE, Mar. 24, 1992. DOI: 10.2118/22405-ms.

[46] Frans Richard Kodong, Herry Sofyan, and Hari Prapcoyo. *IMPLEMENTASI APLIKASI ANDROID-BASED UNTUK PENANGGULANGAN WELL KICK PADA PEMBORAN MINYAK DAN GAS BUMI*. Dec. 15, 2020.

[47] Damilola Ojedeji, Scott Perry, James Nielsen, and Yuanhang Chen. "Experimental investigation of desorption kinetics of methane in diesel and internal olefin for enhanced well control". In: *Greenhouse Gases: Science and Technology* 10.2 (Mar. 20, 2020), pp. 364–379. DOI: 10.1002/ghg.1967.

[48] Robin Beckwith. "SPE Liquids-Rich Basins Conference: New Technology for Old Plays". In: *Journal of Petroleum Technology* 65.11 (Nov. 1, 2013), pp. 106–121. DOI: 10.2118/1113-0106-jpt.

[49] Koray Kinik, Ferhat Gumus, and Nadine Osayande. "Automated Dynamic Well Control With Managed-Pressure Drilling: A Case Study and Simulation Analysis". In: *SPE Drilling & Completion* 30.02 (Apr. 29, 2015), pp. 110–118. DOI: 10.2118/168948-pa.

[50] M Agus Nukman M Mabror et al. "Integrated Operations IO: Production Management System Goes Dynamic Using Online Transient Modelling". In: *SPE Asia Pacific Oil & Gas Conference and Exhibition*. SPE, Oct. 25, 2016. DOI: 10.2118/182497-ms.

[51] Bin Hu, Anne Sofie Olsen, Neal Hewitt, and Michael John Branchflower. "Use Dynamic Simulation to Diagnose the Startup Failure of a Long Horizontal Well in the North Sea". In: *SPE Norway Subsurface Conference*. SPE, Nov. 2, 2020. DOI: 10.2118/200736-ms.